Quasielastic processes in the $^{28}Si+^{208}Pb$ reaction at 8 MeV per nucleon

J. J. Kolata,* K. E. Rehm, D. G. Kovar, G. S. F. Stephans, G. Rosner,† and H. Ikezoe‡
Argonne National Laboratory, Argonne, Illinois 60439

R. Vojtech
Physics Department, University of Notre Dame, Notre Dame, Indiana 46556
(Received 27 March 1984)

Quasielastic yields have been measured for the $^{28}Si+^{208}Pb$ reaction at $E_{lab}(^{28}Si)=225$ MeV. The inelastic scattering is dominated by excitation of the first 2^+ level in ^{28}Si. The angular distribution for this state is found to contain insufficient information to determine accurately the quadrupole deformation parameter once the possibility of hexadecapole deformation is admitted. The ambiguity is resolved by requiring a simultaneous fit to the angular distribution of the first 4^+ state in ^{28}Si. A large fraction of the total reaction cross section is found to be contained in quasielastic neutron transfer, and transfer of a single proton. It is shown that these large quasielastic yields are consistent with the expectations from distorted-wave Born approximation calculations.

I. INTRODUCTION

Recently, it has been observed[1] that quasielastic neutron pickup contributes a large fraction of the total reaction cross section in the interaction of moderately heavy ions (Cl, Ti, and Ni) with ^{208}Pb at incident energies of about 1.25–1.5 times the Coulomb barrier. The corresponding total kinetic energy losses are of the order of 5 MeV. Systematic studies of reactions induced by lighter projectiles such as ^{16}O have shown[2–4] that quasielastic transfer can contribute significantly to the reaction cross section near the Coulomb barrier, but the relative importance of such processes decreases rather rapidly with incident beam energy. In the present experiment, we have investigated the quasielastic transfer yields for the $^{28}Si + ^{208}Pb$ reaction at an energy corresponding to 1.6 times the Coulomb barrier in an attempt to add to the systematics of these observations. In the process, we have also measured the elastic and inelastic scattering, which are of interest since ^{28}Si is strongly deformed ($\beta_2 \approx -0.4$). In principle, the present data can provide detailed information concerning the static and dynamic shape parameters for ^{28}Si, which can be compared with the results from experiments with lighter ions. The effect of introducing hexadecapole deformation into the analysis is emphasized.

II. EXPERIMENTAL METHOD

The experiment was performed using a beam of 225 MeV ^{28}Si ions, of intensity up to 2 particle nA, obtained from the Argonne superconducting linac. The targets consisted of 50 $\mu g/cm^2$ of isotopically enriched (99.86%) ^{208}Pb evaporated onto 15 $\mu g/cm^2$ C foils. The reaction products were momentum analyzed in an Enge split-pole spectrograph, and detected in the focal plane using a position-sensitive ionization chamber.[5] The position, dE/dx, total energy, and angle of incidence were measured for each ion, so that mass and Z identification could be obtained. Energy resolutions of $\approx$400 keV (FWHM) were observed. A typical spectrum of outgoing ^{28}Si ions is shown in Fig. 1. Absolute cross sections were obtained from the elastic scattering data under the assumption that $\sigma_{elast}/\sigma_{Ruth}=1.00$ for $\theta_{c.m.}<25°$. Three charge states were simultaneously measured at each angle, representing more than 80% of the total charge-state distribution. The estimated error in the absolute yield is $\pm 5\%$. Angular distributions obtained for the elastic, inelastic, and transfer channels studied are shown in Figs. 2 and 3.

III. ELASTIC AND INELASTIC SCATTERING

The $^{28}Si + ^{208}Pb$ system presents an interesting challenge due to the fact that, even at 8 MeV per nucleon (corresponding to 1.6 times the Coulomb barrier), the inelastic scattering is dominated by Coulomb excitation of the

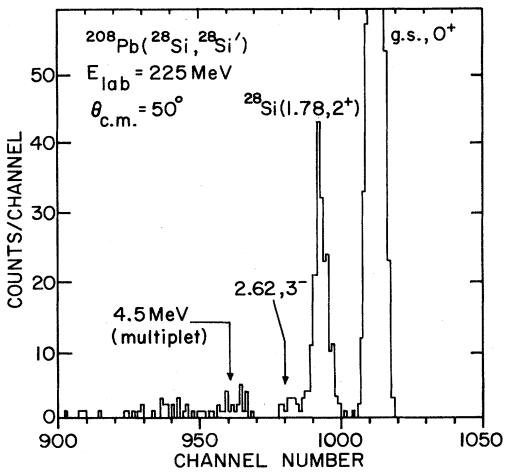

FIG. 1. Spectrum of charge 13^+ ^{28}Si ions from the $^{208}Pb+^{28}Si$ reaction at 225 MeV, taken at a c.m. scattering angle of 50°.

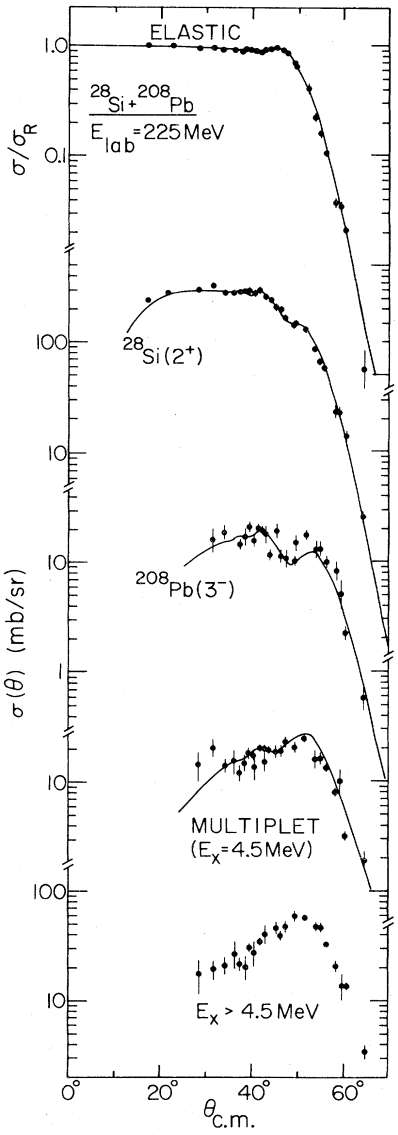

FIG. 2. Angular distributions for elastic scattering and for inelastic scattering to the first 2^+ state in ^{28}Si, the first 3^- state in ^{208}Pb, the multiplet at $E_x = 4.5$ MeV, and to all states above 4.5 MeV as obtained in the present experiment. The solid curves are the result of the ROT3 coupled-channels calculation discussed in the text.

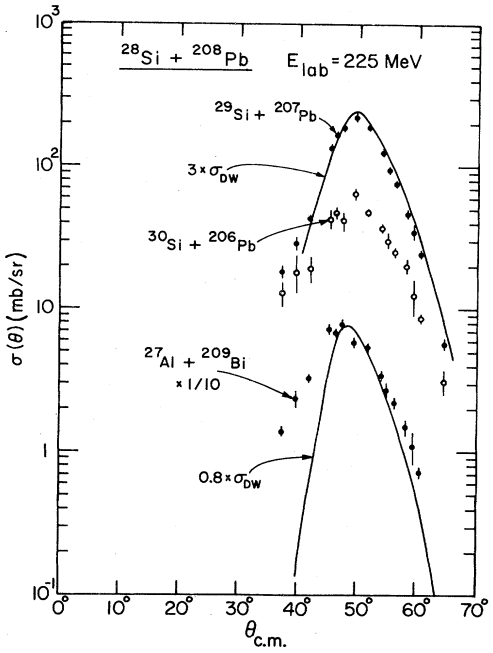

FIG. 3. Angular distributions for one- and two-neutron pick-up and one-proton stripping from the present experiment. The solid curves are the results of the DWBA calculation discussed in the text.

1.778-MeV level in ^{28}Si. The corresponding strong perturbation of the elastic scattering (Fig. 2) implies that a coupled-channels (CC) treatment is essential. The analysis was performed with the coupled-channels version of the program PTOLEMY.[6]

As a first step, we reproduced the results of Christensen *et al.*[7] who analyzed the scattering of ^{28}Si from ^{208}Pb at 210 MeV. The optical-model potential was initially taken to be the four-parameter, large diffuseness VIB2 potential of Ref. 7. However, in order to achieve a good fit to the present data set it was necessary to slightly increase both the radius and the imaginary well depth, resulting in the potential VIB2′ of Table I. (The definition of the optical-model parameters is as in Ref. 4.) With these changes, an excellent fit was obtained to the elastic and ^{28}Si (2^+) angular distributions, equal in quality to that shown in Fig. 2. The "rotational model" calculation described in Ref. 7 was also reproduced. In this model, the deformed optical-model potential is expanded to all orders in spherical harmonics and the quadrupole part is then projected out. This is probably a reasonable description of the reaction since ^{28}Si is known[8] to have a large static quadrupole moment which is essentially equal to the rotational value deduced from the measured $B(E2)$. The optical-model potential obtained is given as ROT2′ in Table I. Again, an excellent simultaneous fit to the elastic and 2^+ angular distributions was obtained.

To go beyond the calculations presented in Ref. 7, we note that ^{28}Si is known to have large positive hexadecapole deformation.[9–12] Calculations were performed using this information, and restricting the treatment of ^{28}Si to the more realistic rotational model while vibrational coupling was used for the $0^+ \leftrightarrow 3^-$ and $0^+ \leftrightarrow 2^+$ transitions in ^{208}Pb. The initial calculations of this kind demonstrated that the ^{28}Si 2^+ angular distribution is most strongly perturbed by the addition of Y_4 deformation in

TABLE I. Optical-model potentials used in the analysis.

Potential	V (MeV)	r_0 (fm)	a (fm)	W (MeV)	r_{0c} (fm)
VIB2′	40.	1.252	0.65	28.67	1.32
ROT2′	40.	1.246	0.65	28.74	1.32
ROT3	40.	1.238	0.65	28.80	1.32

the region of the grazing angle, in this case near $\theta_{c.m.}=50°$. This effect has previously been reported by Gross *et al.*[13] in their analysis of $^{20}Ne+^{208}Pb$ scattering. However, it was also found that excellent simultaneous fits to the elastic and 2^+ inelastic angular distributions could be obtained with a wide variety of hexadecapole deformation parameters β_4 ranging between 0—0.2, provided only that β_2 was also allowed to vary from -0.28 to -0.40. Thus, the 2^+ angular distribution by itself does not contain enough information to accurately determine *either* the quadrupole *or* the hexadecapole deformation in the absence of other information.

Fortunately, additional information is available in the angular distribution to the multiplet at $E_x=4.5$ MeV, which contains transitions to the 4.08 MeV 2^+ level in ^{208}Pb and the 4.62 MeV 4^+ level in ^{28}Si, as well as a level at 4.40 MeV corresponding to mutual excitation of the first 2^+ state in ^{28}Si and the 3^- state in ^{208}Pb. The first of these was resolved in the data of Ref. 7. The 4^+ and mutual-excitation levels, however, were not analyzed. In the present experiment, we were not able to resolve any of these transitions and so a composite angular distribution (Fig. 4) was obtained. The curves in Fig. 4 illustrate the decomposition of this angular distribution into its separate components according to the calculation discussed below. It can be seen that the predicted behavior in the 50°—60° angular range is strongly dependent on the magnitude of the ^{28}Si 4^+ yield. For comparison, we also show in Fig. 4 the prediction for $\beta_4=0$, in which case the

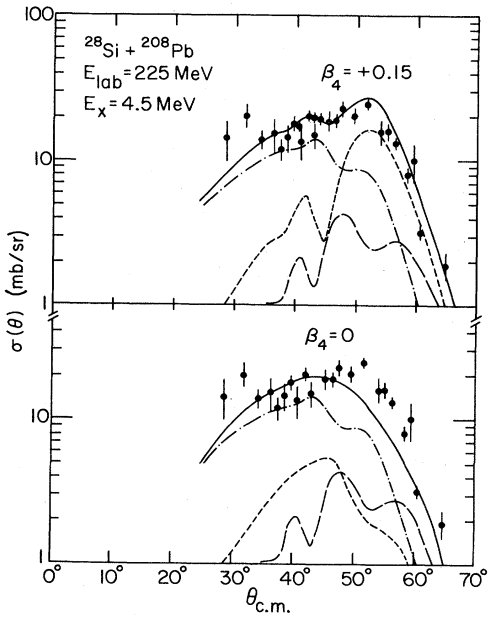

FIG. 4. Angular distribution for inelastic scattering to the multiplet at $E_x=4.5$ MeV obtained in the present experiment. The solid curves illustrate the result of the ROT3 calculation for $\beta_4=0.15$ (upper) and $\beta_4=0$ (lower) with electromagnetic matrix elements as given in Table II. The dashed curves are the computed decomposition of the multiplet into individual angular distributions in the two cases. The dot-dashed curve is the predicted angular distribution for the 2^+ state in ^{208}Pb, the short dashed curve is that for the 4^+ state in ^{28}Si, and the long-dashed curve corresponds to the mutual excitation angular distribution.

population of the 4^+ state occurs primarily by the $0^+\rightarrow2^+\rightarrow4^+$ route with only a small amount of direct $0^+\rightarrow4^+$ excitation coming from the Y_4 projection of the deformed potential.

In the final coupled-channels calculation, the $0^+\leftrightarrow2^+$, $0^+\leftrightarrow4^+$, and $2^+\leftrightarrow4^+$ transitions in ^{28}Si were included, along with the $0^+\leftrightarrow3^-$ and $0^+\leftrightarrow2^+$ transitions in ^{208}Pb. The corresponding electromagnetic matrix elements, given in Table II, were taken from the literature[8,14] and are the same as those used in Ref. 7. (The direct $E4$ transition matrix element for the 4^+ state of ^{28}Si was, however, determined by requiring that the Coulomb and nuclear Y_4 deformation lengths be equal. This leads to the prediction that the ground-state branching ratio for the electromagnetic decay of the 4^+ state is 1.6×10^{-7}.) These matrix elements affect predominantly the forward-angle ($\theta_{c.m.}<40°$) behavior of the inelastic angular distributions for the appropriate states. It can be seen (Fig. 2) that calculations employing the literature values are adequate to account for the present data. Mutual excitation of the 2^+ state in ^{28}Si and the 3^- state in ^{208}Pb was allowed to occur through the $0^+\leftrightarrow2^+\leftrightarrow$mutual and $0^+\leftrightarrow3^-\leftrightarrow$mutual multistep routes, as well as directly via the simultaneous excitation of the two states. No other couplings between states in ^{28}Si and states in ^{208}Pb were included. Reorientation of the 2^+ state in ^{28}Si via $l=2$ and 4 coupling was allowed. An intrinsic quadrupole moment $Q_0=-58$ e fm^2, taken from the literature,[8] was assumed. A calculation using $Q_0=0$ showed that the reorientation effect was important, but that the present data could not provide a better estimate than the literature value. Reorientation effects in all other states were ignored, since (i) the static quadrupole moment of ^{208}Pb is small, (ii) the back coupling of reorientation in the 4^+ state of ^{28}Si on the 2^+ angular distribution is of higher order, and (iii) the effect of reorientation on the 4^+ angular distribution is expected to be smaller than the error due to neglect of coupling to other states in ^{28}Si, particularly the 6^+ state. The complete coupling scheme is illustrated in Fig. 5, and the results of the calculation with $\beta_2=-0.36$, $\beta_4=+0.15$ for ^{28}Si, and $\beta(3^-)=0.09$, $\beta(2^+)=0.06$ for ^{208}Pb are shown in Fig. 2. It can be seen that excellent simultaneous fits are obtained to all angular distributions, after slight adjustment of the optical-model potential to obtain the set ROT3 in Table I. The need for such an adjustment was anticipated due to the fact that more states are explicitly coupled in this scheme.

TABLE II. Electromagnetic matrix elements and deformation lengths for ^{208}Pb transitions.

States	$\langle f\|\|E_\lambda\|\|i\rangle$ (e fm$^\lambda$)	δ_λ (fm) VIB2[a]	δ_λ (fm) Present work
^{28}Si (2^+-0^+)	-18.06		
^{28}Si (4^+-0^+)	140.		
^{28}Si (4^+-2^+)[b]	$-25.$		
^{208}Pb (3^--0^+)	816.	0.56(8)	0.64(10)
^{208}Pb (2^+-0^+)	55.	0.43(6)	0.43

[a] Reference 7.
[b] For $\lambda=2$.

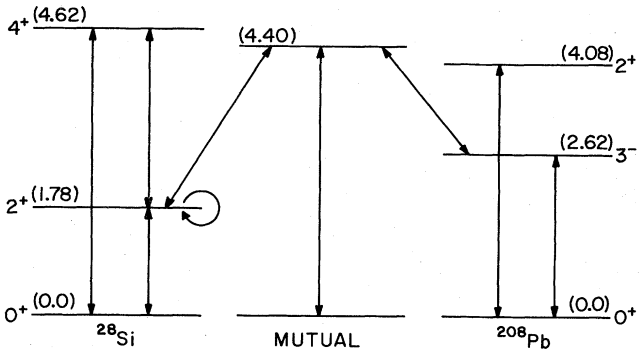

FIG. 5. Complete coupling scheme for the ROT3 calculation. All states, transitions, and reorientation couplings included in the calculation are illustrated. The excitation energy of each state in MeV is given in parentheses.

The deformation parameter $\beta=0.09$ obtained for the 3^- state in ^{208}Pb corresponds to a deformation length $\delta_3=0.64$ fm (where $\delta=\beta R_A$, with R_A being the radius of the nucleus involved). This is slightly larger than the value of 0.56 fm given in Ref. 7. The primary effect of this change in δ_3 was to improve the agreement with the experimental data in the region from $\theta_{\text{c.m.}}=55°$ to 65°. The deformation length for the 2^+ state in ^{208}Pb was taken to be identical to that given in Ref. 7 ($\delta_2=0.43$ fm). No independent measure of this parameter could be obtained because of the fact that the 2^+ state was unresolved in the present experiment.

The deformation parameters for ^{28}Si obtained in several different experiments are given in Table III. The assigned errors on these quantities from the present experiment reflect the range over which an acceptable fit could be obtained to the composite angular distribution of the multiplet at $E_x=4.5$ MeV, as well as an estimate of the effect of coupling to states not included in the present calculation (such as the 6^+ state in ^{28}Si), and of the reorientation of the 4^+ state in ^{28}Si. In comparison with the results quoted by Christensen *et al.*,[7] note that inclusion of hexadecapole distortion forces the quadrupole deformation parameters toward larger absolute value (more oblate shape) so that the inferred deformation length is greater than or equal to that measured in an α-scattering experiment (Ref. 11). Furthermore, the Y_4 deformation length as deduced from the present experiment is also greater than or equal to the (α,α') value. As has been emphasized by Hendrie,[16] however, the comparison of deformation lengths results in only a first order correction of effects due to the finite size of the target or projectile. Intrinsic deformations for ^{28}Si deduced within the context of the "rolling model" (Ref. 16) are compared in Table IV. It can be seen that, within experimental error, the corrected deformation lengths agree.

TABLE IV. Deformation lengths of ^{28}Si according to the rolling model.

Probe	δ_2 (fm)	δ_4 (fm)	δ_6[a] (fm)
^{208}Pb	−1.70(19)	0.82(27)	−0.25
(α,α')	−1.65(5)	0.50(7)	−0.30
(p,p')	−1.48	1.24(41)	−0.23

[a] Generated from the rolling model under the assumption that the *observed* value of δ_6 was zero.

IV. TRANSFER PROCESSES

One of the more interesting results of the present experiment is the observation that few-neutron transfer processes exhaust a significant fraction of the total reaction cross section for ^{28}Si+^{208}Pb at this energy. For example, the excitation-energy-integrated angular distribution for one neutron pickup (Fig. 3) corresponds to a total yield of 214±2 mb. Similarly, the two-neutron pickup cross section is 60±10 mb, and the single-proton stripping yield is 80±2 mb. These may be compared with a total reaction cross section (defined to exclude the largely Coulomb-excited yield of the ^{28}Si first 2^+ state) of 2260 mb from

TABLE III. Deformation parameters for ^{28}Si.

Probe	β_2	δ_2 (fm)	β_4	δ_4 (fm)	Q_0 (e fm^2)	Ref.
^{208}Pb[a]	−0.36(4)	−1.37(15)	+0.15(5)	+0.6(2)	−58[b]	Present work
^{208}Pb[c]	−0.28(4)	−1.06(16)			−58[b]	7
^{58}Ni	−0.38	−1.37			−58[b]	15
(α,α')	−0.32(1)	−1.20(4)	+0.08(1)	+0.30(4)	−52	11
(α,α')[d]	−0.39(1)	−1.42(4)	+0.27(3)	+0.98(11)	−56	12
(p,p')[e]	(−)0.34	(−)1.28	+0.25(8)	+0.9(3)	(−)54	10
(e,e')	−0.39	−1.47	+0.10	+0.4	−64(3)	9

[a] ROT3 calculation. Values given in parentheses indicate assigned errors in the least significant digit(s). See the text for further discussion of the assigned errors in the present experiment.
[b] Value (magnitude and sign) taken from the literature (Ref. 8).
[c] VIB2 parameter set.
[d] Folding-model analysis of the data in Ref. 11 (see previous line). Note the large increases in the magnitudes of δ_2 and δ_4 from this analysis.
[e] Parentheses around the sign indicate an assumed phase.

the coupled-channels analysis or 2178 mb from the "sum-of-differences" (SOD) method[17,18] (Fig. 6). The latter is a purely empirical procedure for obtaining the reaction cross section from the difference $\Delta(\theta)$ between Rutherford scattering and the observed elastic cross section. In the present case, because the strong Coulomb excitation of the $^{28}Si(2^+)$ state causes large deviations from Rutherford scattering even at angles far below the grazing peak, we found it expedient to add the elastic and 2^+ inelastic yields prior to calculating $\Delta(\theta)$. The resulting SOD integrand $[2\pi \sin\theta\Delta(\theta)]$, shown in Fig. 6, is assumed to be zero below the angle θ_{min}, and its integral gives directly the total reaction cross section minus the 2^+ yield. In either case, the summed yield of the above transfer channels is found to contribute 16% of the total reaction cross section. Furthermore, the bell-shaped angular distribution (Fig. 3) and relatively low excitation energies in the residual system (Fig. 7) suggest a peripheral quasielastic reaction mechanism. By way of comparison, the nuclear part of the inelastic scattering to the states considered in the CC calculation discussed above is only 78 mb, i.e., 3.5% of the total reaction cross section. The integrated yield to inelastic states above $E_x=4.5$ MeV (Fig. 1) is 100 ± 5 mb, but part of this cross section possibly results from Coulomb excitation or from neutron transfer followed by evaporation. Thus, we estimate that nuclear inelastic scattering accounts for 7 ± 2 % of the total reaction cross section at this energy, and that this channel is only about 75% as strong as the 1n transfer process.

It would clearly be of interest to perform a CC calculation in which the observed strong quasielastic transfer channels are explicitly taken into account, together with the inelastic routes discussed above. Unfortunately, this is not possible with current finite-range CC codes, so that one must resort to the DWBA instead. One important question then becomes the choice of the optical-model potential to be used. In the standard DWBA calculation, the

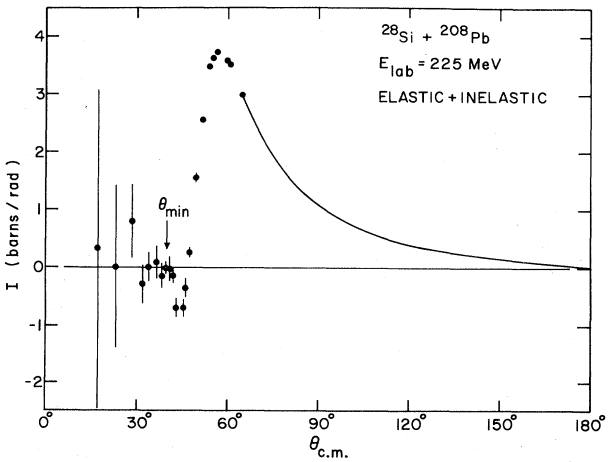

FIG. 6. Sum-of-differences (Refs. 17 and 18) integrand determined from the sum of the elastic plus ^{28}Si (2^+) inelastic angular distributions. The solid curve corresponds to the Rutherford cross section multiplied by $\sin\theta$. Integration of this data from θ_{min} to 180° yields a total reaction cross section of 2178 mb.

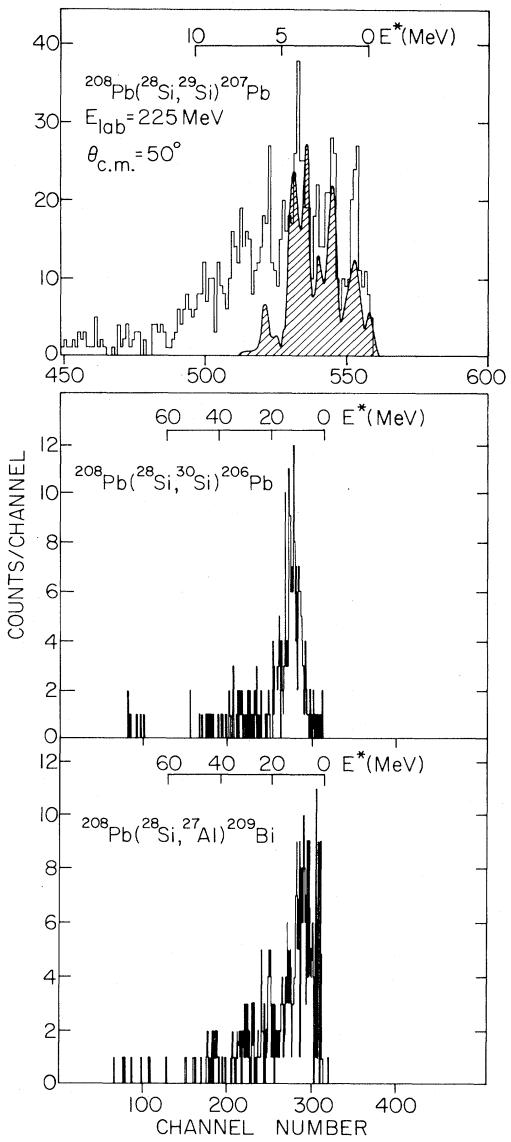

FIG. 7. Excitation-energy distribution of the transfer strengths at the grazing angle. The shaded curve is the result of the ROT3 calculation. The experimental energy resolution of 400 keV (FWHM) has been folded into this calculation.

parameters of this potential are determined from fits to the elastic scattering data. Because coupling to the ^{28}Si first 2^+ state strongly perturbs the elastic angular distribution, this prescription cannot be followed in the present case. Instead, we use[19] the "reference potential" ROT3 which resulted from the CC analysis. The *same* potential is used in both the entrance and exit channels, although it is known[20] that the deformation parameters change rather rapidly with neutron and proton number in this mass region. It should also be noted that, at least for ^{29}Si, the exit channel is strongly coupled[21] to the first 2^+ state in ^{28}Si.

Single-neutron and single-proton transfer form factors were obtained by binding the appropriate particles at the correct separation energies for the target and projectile, in a spherical Woods-Saxon well with radius parameter

TABLE V. Shell-model states and spectroscopic factors used in the DWBA calculations.

Nuclide	State	E_x	C^2S	Ref.	Nuclide	State	E_x	C^2S	Ref.
^{29}Si	$2s_{1/2}$	0.0	0.32	8,20	^{207}Pb	$3p_{1/2}$	0.0	2.14	22
^{29}Si	$1d_{3/2}$	1.273	0.69	8,20	^{207}Pb	$2f_{5/2}$	0.570	6.80	22
^{29}Si	$1d_{5/2}$	2.032	0.16	8,20	^{207}Pb	$3p_{3/2}$	0.890	4.00	22
^{29}Si	$1d_{5/2}$	3.069	0.12	8,20	^{207}Pb	$1i_{13/2}$	1.633	14.5	22
^{29}Si	$1f_{7/2}$	3.623	0.45	8,20	^{207}Pb	$2f_{7/2}$	2.340	7.10	22
					^{207}Pb	$1h_{9/2}$	3.413	9.8	22
^{27}Al	$1d_{5/2}$	0.0	3.39	8	^{209}Bi	$1h_{9/2}$	0.0	1.00	23
^{27}Al	$2s_{1/2}$	0.843	0.79	8	^{209}Bi	$2f_{7/2}$	0.896	1.04	23
^{27}Al	$1d_{3/2}$	1.013	0.48	8	^{209}Bi	$1i_{13/2}$	1.608	1.01	23
^{27}Al	$1d_{5/2}$	2.732	0.41	8	^{209}Bi	$2f_{5/2}$	2.822	0.91	23
^{27}Al	$1d_{3/2}$	2.980	0.53	8	^{209}Bi	$3p_{3/2}$	3.118	0.90	23
^{27}Al	$1p_{1/2}$	4.055	1.51	8	^{209}Bi	$3p_{1/2}$	4.421	0.46	23
^{27}Al	$1d_{5/2}$	4.409	0.29	8	^{209}Bi	$2f_{7/2}$	4.447	0.16	23
^{27}Al	$1p_{3/2}$	5.155	1.36	8					

$r_0=1.20$ fm, diffuseness $a=0.65$ fm, and spin-orbit well depth $V_{so}=7$ MeV. The single particle states considered in the analysis, together with their excitation energies and spectroscopic factors as determined from light-ion transfer experiments,[8,21–23] are given in Table V. In both cases, these states include all known levels with large spectroscopic factor [$C^2S>0.1$ or $C^2S>0.1(2j+1)$] in the region from 0–5 MeV of excitation in either nucleus.

The angular distribution for single-neutron pickup from the calculation described above is shown in Fig. 3, where the predicted yield has been multiplied by a factor of 3 to allow comparison with the experimental angular distribution. The bell shape is nicely reproduced. The absolute yield is much smaller than experimentally observed, but transfer to states at high excitation having small or poorly determined spectroscopic strengths has not been included. Comparing the predicted and observed excitation-energy distribution of transfer strength (Fig. 7), it can be seen that a good part of the discrepancy can be traced to such states. Confining the comparison to configurations within the first 5 MeV of excitation, the ratio of experiment to theory is 1.5. Furthermore, the predicted and observed transfer-strength distributions in this energy region (Fig. 7) bear a striking resemblance to one another. (The theoretical prediction in this figure was obtained by Gaussian folding of the strength distribution for the 30 states considered between 0–7 MeV of excitation, using the experimental energy resolution of 400 keV.) We conclude that the DWBA calculation, despite its limitations, does a reasonably good job of accounting for the observed large quasielastic neutron transfer yield.

In relating these neutron transfer data to the results of Ref. 1, we note that $\sigma_{1n}/\sigma_{reac}=0.098$ and $\sigma_n/\sigma_{reac}=0.126$, values which are similar to those observed for ^{37}Cl+^{208}Pb at $E/V_{Coul}=1.4$ (0.088 and 0.139, respectively) and substantially greater than the corresponding ratios for ^{16}O+^{208}Pb at $E/V_{Coul}=1.7$ (0.046 for both). Taking into account the ground-state Q values, the 1n and 2n transfer centroids in the present experiment correspond to total kinetic energy losses of 4 and 6 MeV, respectively, essentially identical to the effective Q value of -5 MeV obtained[1] for Ni-induced reactions on ^{208}Pb. The experimental optimum Q values for several of the particle transfer channels measured in the present work are shown in Fig. 8, together with their associated "Q window" widths. The dot-dash curve in this figure corresponds to the prediction of a semiclassical model[24] based on the matching of Coulomb trajectories and including the effect of "recoil," i.e., the shift in the center of mass of the two nuclei at the instant of transfer. The observed total kinetic energy losses are substantially underpredicted in this

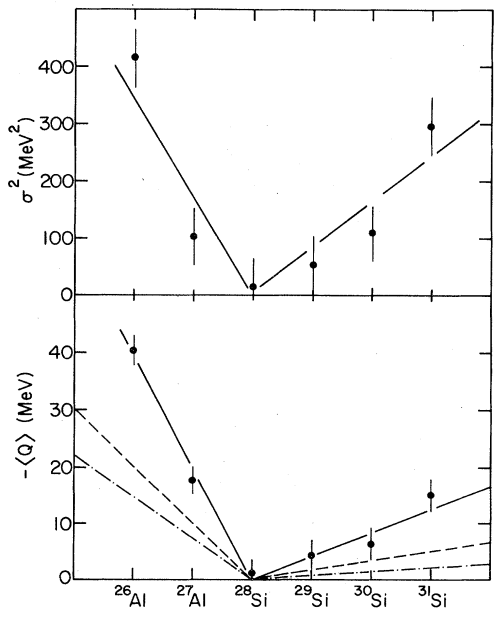

FIG. 8. Experimental and predicted optimum Q values for neutron pickup and proton-stripping reactions observed in this experiment. The solid curve reproduces the trend of the experimental data, the dash-dot curve is the semiclassical result, and the dashed curve is a DWBA prediction. See the text for a further discussion. Also illustrated are the experimental widths of the "Q window" for each of the reactions.

model. Also illustrated in Fig. 8 (dashed curve) is the result of a DWBA calculation with parameters as described above, and for transferred angular momentum $L=0-5\hbar$. No dependence of Q_{opt} on L was observed for this range of angular momentum. It can be seen that discrepancies remain, though reduced in magnitude from the semiclassical estimates. Similar results have been obtained by Henning *et al.*,[25] among others. Finally, we observe that the DWBA calculations for 1n transfer are in reasonable accord with the experimental data at low excitation energy, as in Ref. 1. The energy resolution obtained in the present work, however, allows a more detailed comparison of experiment and theory to be made.

The predicted differential cross section for single-proton stripping (Fig. 3) is substantially smaller than the experimental yield at angles below grazing. Note also that the calculation has here been multiplied by a factor of 8

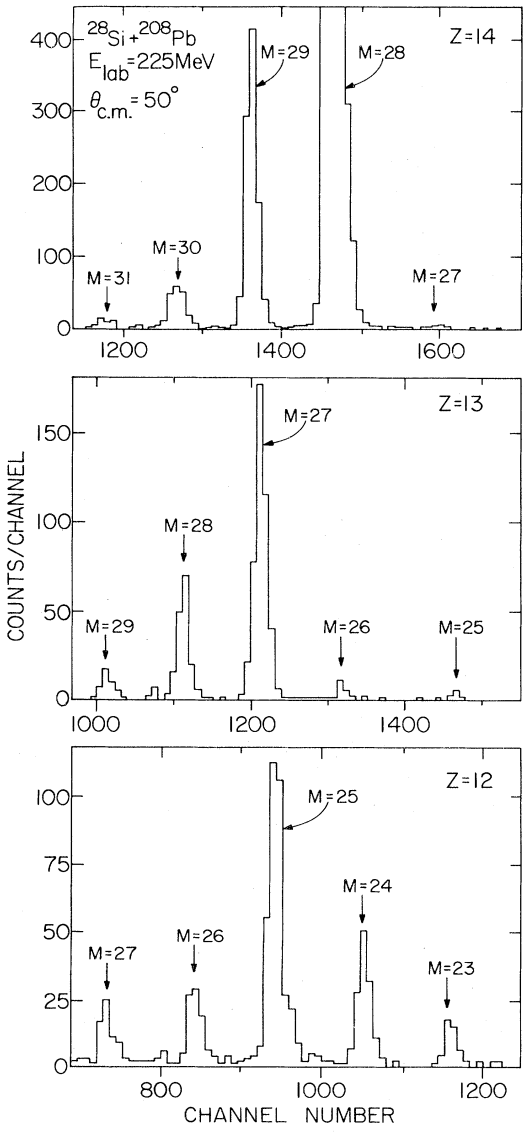

FIG. 9. Mass spectra for Si, Al, and Mg ions at $\theta_{c.m.}=50°$, as obtained in the present experiment.

rather than 3 as in the neutron-transfer case. On the other hand, considering only the first 5 MeV of excitation where all the relevant states have been included in the calculation, the ratio of experiment to theory is 1.6, i.e., approximately equal to that observed for single-neutron pickup.

The centroid of the single-proton-transfer strength corresponds to a total kinetic energy loss of 17.5 MeV, considerably greater than the 5 MeV deduced from the neutron transfer data. However, in the case of charge transfer the dominant effect on the optimum Q value comes from the Coulomb potential, and we estimate $Q_{opt}=-(8-10)$ MeV (Fig. 8). The difference in optimum Q value explains the fact that 52% of the neutron transfer strength at the grazing angle is observed below 5 MeV of excitation, whereas the corresponding value for proton transfer is only 22%. With regard to other transfer channels, the mass spectra for $Z=Q=12-14$, where Q is the charge state of the ion, are shown in Fig. 9. (Note, however, that there is a $\Delta M=4$ ambiguity due to the fact that ^{31}Si in the 14^+ charge state has a very similar Q^2/M ratio to that of ^{27}Si in the 13^+ charge state, for example. Thus, the highest-mass peak for each Z in Fig. 9 has some contributions from ions of a different mass and charge state.) Considering first the mass distribution of Si isotopes, note that neutron pickup is strongly preferred over neutron stripping, consistent with the fact that the pickup Q value is more positive by 14 MeV. In the case of proton transfer, the proton stripping channel (^{27}Al) is relatively strong, whereas we observed virtually no proton pickup (^{29}P) yield

$$\left[\frac{d\sigma}{d\Omega_{peak}}<0.5\ \text{mb/sr}\right].$$

In this case, the predicted Q_{opt} for proton pickup is 8—10 MeV, but the ground-state Q value is -5.3 MeV. Finally, the relatively large yields of ^{28}Al and ^{25}Mg are of some interest, since these nuclides (most likely predominantly produced via proton and α-particle evaporation from highly excited states in ^{29}Si) provide an indication of the importance of sequential processes. There appears to be little evidence for large, direct α-particle transfer cross sections.

V. SUMMARY AND CONCLUSIONS

Quasielastic yields have been measured for the $^{28}Si+^{208}Pb$ reaction at $E_{lab}(^{28}Si)=225$ MeV, corresponding to 1.6 times the Coulomb barrier for this system. Analysis of the inelastic scattering to the first 2^+ state in ^{28}Si, in the context of the CC, has shown that this angular distribution by itself does not contain enough information to accurately determine either the quadrupole or the hexadecapole deformation in the absence of other information. Specifically, the elastic and 2^+ inelastic data can be simultaneously fit with a wide range of hexadecapole deformations, provided only that the quadrupole deformation parameter is allowed to vary within reasonable limits. Our analysis indicates that this ambiguity can be resolved by also requiring a simultaneous fit to the 4^+ state in ^{28}Si. The magnitude of the resulting quadrupole deformation

length is 40% greater than that deduced under the assumption of zero Y_4 deformation.[7] It is also similar to the value obtained from inelastic proton[10] and α-particle[11] scattering, and the Y_4 deformation length is also similar to the corresponding (α,α') value. In the context of the rolling model of Hendrie, corrected ^{28}Si deformation lengths appear to agree within experimental error for data taken with a wide variety of hadronic probes.

With regard to a further extension of this work, it would certainly be of interest to obtain sufficient experimental resolution to completely separate the crucial 4^+ state from other nearby states. Another possibility would be to try a different class of optical model potential, other than the 40-MeV deep, large diffuseness Woods-Saxon well used. It has been noted,[7] however, that this potential is very close to the folding-model potential derived to fit lower-energy ^{28}Si+^{208}Pb data.[26] Finally, it would be of some interest to investigate the effect of coupling of the inelastic states to the strong quasielastic transfer channels, especially since it is known[21] that several of the states in ^{29}Si have large parentage from single neutrons coupled to the first 2^+ excitation in ^{28}Si. This effect, if large, would have clear implications for experiments designed to measure deformation parameters by inelastic heavy-ion scattering, particularly since strong quasielastic neutron transfer appears to be a rather general feature in reactions induced by moderately heavy ions.

In the present experiment, we have found that 1n, 2n, and 1p quasielastic transfer channels contribute 16% of the total reaction cross section for ^{28}Si+^{208}Pb at 8 MeV per nucleon. A further 7% is contained in the nuclear part of the inelastic scattering yield. The large neutron pickup cross sections are consistent with the observations made in Ref. 1, while large quasielastic proton stripping yields have apparently not been reported previously for medium-mass heavy-ion reactions. Distorted-wave Born approximation calculations were found to reproduce the single-particle transfer cross sections to states at low excitation ($\lesssim 5$ MeV) to within a factor of 1.5, and the observed distribution of transfer strength to these states is also well reproduced. The 1n and 2n transfer centroids correspond to total kinetic energy losses of 4 and 6 MeV, respectively, as compared to 5 MeV obtained for Ni-induced reactions on ^{208}Pb. The centroid of the 1p transfer strength corresponds to the much larger value of 17.5 MeV, as expected for a charge-transfer reaction. The comparisons with DWBA calculations show that large quasielastic yields are not unexpected, at least for 1n and 1p transfers to the excitation-energy region (0—5 MeV) for which relatively complete calculations were possible.

ACKNOWLEDGMENTS

One of the authors (J.J.K.) would like to acknowledge the help of S. C. Pieper in carrying out the CC calculations. This work was partially supported by US DOE Contract W-31-109-Eng-38 and by the US NSF under Grant No. PHY82-00426.

*Permanent address: Physics Department, University of Notre Dame, Notre Dame, IN 46556.

†Present address: Physik-Department E12, Technische Universitat München, James-Franck-Strasse, D-8046 Garching, Federal Republic of Germany.

‡Present address: Japan Atomic Energy Research Institute, Tokai Research Establishment, Tokai Naka-Gun, Ibaraki-Ken, Japan.

[1]K. E. Rehm, D. G. Kovar, W. Kutschera, M. Paul, G. Stephans, and J. L. Yntema, Phys. Rev. Lett. **51**, 1426 (1983).

[2]W. Henning, J. P. Schiffer, D. G. Kovar, S. Vigdor, B. Zeidman, Y. Eisen, and H. J. Körner, Phys. Lett. **58B**, 129 (1975).

[3]F. Videbaek, R. B. Goldstein, L. Grodzins, S. G. Steadman, T. A. Belote, and J. D. Garrett, Phys. Rev. C **15**, 954 (1977).

[4]S. C. Pieper, M. H. Macfarlane, D. H. Gloeckner, D. G. Kovar, F. D. Becchetti, B. G. Harvey, D. L. Hendrie, H. Homeyer, J. Mahoney, F. Pühlhofer, W. von Oertzen, and M. S. Zisman, Phys. Rev. C **18**, 180 (1978).

[5]J. R. Erskine, T. H. Braid, and J. G. Stoltzfus, Nucl. Instrum. Methods **135**, 67 (1976).

[6]M. H. Macfarlane and S. C. Pieper, Argonne National Laboratory Report No. ANL-76-11 (Rev. 1), 1978 (unpublished); M. J. Rhoades-Brown, S. C. Pieper, and M. Macfarlane, Phys. Rev. C **21**, 2417 (1980).

[7]P. R. Christensen, S. Pontoppidan, F. Videbaek, J. Barrette, P. D. Bond, Ole Hansen, and C. E. Thorn, Phys. Rev. C **29**, 455 (1984).

[8]P. Endt and C. Van der Leun, Nucl. Phys. **A310**, 1 (1983).

[9]Y. Horikawa, Y. Torizuka, A. Nakada, S. Mitsunoba, K. Kojima, and M. Kimura, Phys. Lett. **36B**, 9 (1971).

[10]R. de Swiniarski, C. G. Glashausser, D. L. Hendrie, J. Sherman, A. D. Bacher, and F. A. McClatchie, Phys. Rev. Lett. **23**, 317 (1969).

[11]H. Rebel, G. W. Schweimer, G. Schatz, J. Specht, R. Löhken, G. Hauser, D. Habs, and H. Klewe-Nebenius, Nucl. Phys. **A182**, 145 (1972).

[12]H. Rebel and G. W. Schweimer, Z. Phys. **262**, 59 (1973).

[13]E. E. Gross, T. P. Cleary, J. L. C. Ford, Jr., D. C. Hensley, and K. S. Toth, Phys. Rev. C **17**, 1665 (1978).

[14]J. S. Lilley, M. A. Franey, and D. M. Feng, Nucl. Phys. **A342**, 165 (1980); J. F. Ziegler and G. A. Peterson, Phys. Rev. **165**, 1337 (1968).

[15]P. D. Bond, Ole Hansen, C. E. Thorn, M. J. LeVine, P. R. Christensen, S. Pontoppidan, F. Videbaek, Jiang Cheng-Lie, and M. J. Rhoades-Brown, Phys. Lett. **114B**, 423 (1982).

[16]D. L. Hendrie, Phys. Rev. Lett. **31**, 478 (1973).

[17]J. T. Holdeman and R. M. Thaler, Phys. Rev. Lett. **14**, 81 (1965); Phys. Rev. **139**, B1186 (1965).

[18]H. Wojciechowski, D. E. Gustafson, L. R. Medsker, and R. H. Davis, Phys. Lett. **63B**, 413 (1976); H. Wojciechowski, L. R. Medsker, and R. H. Davis, Phys. Rev. C **16**, 1767 (1977).

[19]R. J. Ascuitto, J. F. Peterson, and E. A. Seglie, Phys. Rev. Lett. **41**, 1159 (1978).

[20]D. Schwalm, A. Bamberger, P. G. Bizzeti, B. Povh, G. A. P. Englebertink, J. W. Olness, and E. K. Warburton, Nucl. Phys. **A192**, 449 (1972).

[21]H. Clement, R. N. Boyd, C. R. Gould, and T. B. Clegg, Nucl. Phys. **A339**, 285 (1980).
[22]M. R. Schmorak, Nucl. Data Sheets **22**, 487 (1977).
[23]M. J. Martin, Nucl. Data Sheets **22**, 545 (1977).
[24]J. P. Schiffer, H.-J. Körner, R. H. Siemssen, K. W. Jones, and A. Schwarzschild, Phys. Lett. **44B**, 47 (1973).
[25]W. Henning, Y. Eisen, H.-J. Körner, D. G. Kovar, J. P. Schiffer, S. Vigdor, and B. Zeidman, Phys. Rev. C **17**, 2245 (1978).
[26]J. S. Eck, T. R. Ophel, P. D. Clark, D. C. Weisser, and G. R. Satchler, Phys. Rev. C **23**, 228 (1981).